Proximity extracellular protein-protein interaction analysis of EGFR using AirID-conjugated fragment of antigen binding

Kohdai Yamada (koudai072963@gmail.com)
Ehime University
Ryouhei Shioya (ryohei.shioya2515@gmail.com)
Ehime University
Kohei Nishino (k_nishino@tokushima-u.ac.jp)
Tokushima University
Hirotake Furihata (furihata.hirotake.co@ehime-u.ac.jp)
Ehime University https://orcid.org/0000-0002-0171-6751
Atsushi Hijikata (hijikata@toyaku.ac.jp)
Tokyo University of Pharmacy and Life Sciences
Mika Kaneko (mika.kaneko.d4@tohoku.ac.jp)
Tohoku University Graduate School of Medicine
Yukinari Kato (yukinari.kato.e6@tohoku.ac.jp)
Tohoku University
Tsuyoshi Shirai (t_shirai@nagahama-i-bio.ac.jp)
Nagahama Institute of Bio-Science and Technology https://orcid.org/0000-0002-2506-5738
Hidetaka Kosako (kosako@tokushima-u.ac.jp)
Tokushima University https://orcid.org/0000-0003-3228-6368
Tatsuya Sawasaki (sawasaki@ehime-u.ac.jp)
Ehime University https://orcid.org/0000-0002-7952-0556

Article

Keywords:

DOI: https://doi.org/

Additional Declarations: There is **NO** Competing Interest.

Proximity extracellular protein-protein interaction analysis of EGFR using AirID-conjugated fragment of antigen binding

Kohdai Yamada[1], Ryouhei Shioya[1], Kohei Nishino[2], Hirotake Furihata[1], Atsushi Hijikata[3], Mika K Kaneko[4], Yukinari Kato[4,5], Tsuyoshi Shirai[6], Hidetaka Kosako[2*], and Tatsuya Sawasaki[1*]

[1] Division of Cell-Free Life Science, Proteo-Science Center, Ehime University, 3 Bunkyo-cho, Matsuyama, Ehime 790-8577, Japan. [2]Division of Cell Signaling, Fujii Memorial Institute of Medical Sciences, Tokushima University, Tokushima 770-8503, Japan. [3]Laboratory of Computational Genomics, School of Life Sciences, Tokyo University of Pharmacy and Life Sciences, Hachioji, 192-0392, Japan. [4]Department of Antibody Drug Development, Tohoku University Graduate School of Medicine, Sendai, 980-8575, Japan. [5]Department of Molecular Pharmacology, Tohoku University Graduate School of Medicine, Sendai, 980-8575, Japan. [6]Department of Bioscience, Nagahama Institute of BioScience and Technology, 1266 Tamura, Nagahama, 526-0829, Japan.

*Corresponding Authors:

Tatsuya Sawasaki

Proteo-Science Center, Ehime University, Matsuyama 790-8577, Japan

Tel: 81-89-927-8530

Fax: 81-89-927-9941

E-mail: sawasaki@ehime-u.ac.jp.

Hidetaka Kosako

Fujii Memorial Institute of Medical Sciences, Tokushima University, Tokushima 770-8503, Japan

Tel: 81-88-634-6413

Fax: 81-88-634-6405

E-mail: kosako@tokushima-u.ac.jp

Abstract

Receptor proteins, such as epidermal growth factor receptor (EGFR), interact with other proteins in the extracellular region of the cell membrane to drive intracellular signalling. Therefore, analysis of extracellular protein-protein interactions (exPPIs) is important for understanding the biological function of receptor proteins. Here, we demonstrate a new approach using a proximity biotinylation enzyme (AirID) fusion fragment of antigen binding (FabID) to analyse the proximity exPPIs of EGFR. AirID was C-terminally fused to the Fab fragment against EGFR (EGFR-FabID), which could then biotinylate the extracellular region of EGFR in several cell lines. LC-MS/MS analysis indicated that many known EGFR interactors were identified as proximity exPPIs, along with many new candidate interactors, using EGFR-FabID. Interestingly, these proximity exPPIs were influenced by treatment with EGF ligand and its specific kinase inhibitor, gefitinib. These results indicate that FabID provides accurate proximity exPPI analysis of target receptor proteins on cell membranes with ligand and drug responses.

Introduction

Membrane proteins account for more than 30% of the human proteome and play important roles in many cellular functions, such as environmental responses, signal transduction, and cell-cell interactions[1,2]. Additionally, the extracellular regions of many membrane proteins interact with other proteins for these cellular functions[3]. Therefore, analysis of extracellular protein-protein interactions (exPPIs) is a key issue for understanding the biological functions of membrane proteins. General methods to identify proteins interacting with the target protein include the yeast two-hybrid system[4,5], mass spectrometry analysis after immunoprecipitation[6,7], and cell-free protein arrays[8,9]. However, these methods are not suitable for the exPPI analysis of membrane proteins because they have been designed specifically for the analysis of soluble proteins localised in the cytoplasm and nucleus. In addition, because many extracellular regions make specific specialised structures on the membrane and extracellular environments, exPPI analysis requires an environment similar to that of the cell membrane.

When considering the exPPI of membrane proteins, it is important to note that the environment is vastly different outside and inside the cell membrane. Furthermore, the biological responses of membrane proteins, such as ligand binding and cell-cell interactions, occur in the extracellular region of the cell membrane. However, because the extracellular domains of many membrane proteins function as regulatory and response regions for

localisation, transport, and ligand binding, using the native protein without a detectable peptide tag or insertion protein is the best way to perform exPPI analysis. Under these conditions, some studies have used a highly specific monoclonal antibody (mAb) against the extracellular domains of the target membrane protein[10,11] because unnatural modifications are not required, and they can be used directly for cell analysis.

Proximity-labelling technology has been widely used to identify partner proteins[12,13]. Since proximity labelling detects proteins that are very close together, it possibly obtains more precise information about interacting proteins[15,16]. Currently, several proximity-labelling-based techniques, such as the enzyme-mediated proximity cell labelling system (EXCELL)[17], pupylation-based interaction tagging (PUP-IT)[18], engineered ascorbate peroxidase (APEX)[19,20], and μMap, have been developed for the interactome analysis of membrane proteins[10]. These technologies were conjugated to proximity-labelling probes for a target-specific mAb. However, because these methods did not identify the labelling sites, it is not clear whether the interaction regions between the target membrane protein and interacting proteins were exPPIs.

BioID (proximity-dependent biotin identification)[21-24] has been developed as an enzymatic proximity-labelling technology. Recently, we developed a new enzyme AirID for the BioID method[24,25]. However, currently, BioID has not been conjugated to mAb and is used as a direct tool to analyse exPPIs through genetic insertions[26].

In this study, we used a specific AirID-fusion antibody for exPPI analysis of epidermal growth factor receptor (EGFR) in cancer cell lines. AirID was fused to the fragment of antigen binding (Fab) of an antibody because the biotinylation efficiency of FabID to antigens was higher than that of AirID-fusion IgG (mAbID) *in vitro* and in cells. LC-MS/MS analysis of biotinylated peptides indicated that EGFR-FabID biotinylated the extracellular regions of many membrane proteins, including well-known EGFR interactors. Gefitinib (Iressa), a pharmaceutical compound widely used for the treatment of lung cancer, is a highly specific EGFR inhibitor for tyrosine kinase activity in the intracellular region[27]. Interestingly, these proximity exPPI interactions were influenced by the EGF ligand and gefitinib treatment, suggesting that ligand binding and inhibition of receptor tyrosine kinase (RTK) activity have the potential to change exPPIs. These results indicate that the FabID system is a useful method for exPPI analysis of receptor proteins.

Results

Biotinylation of antigen having an epitope AGIA tag by AGIA-mAbID or AGIA-FabID

We recently created a new proximity biotinylation enzyme, AirID, for the BioID method, based on an artificial intelligence algorithm[24]. Because AirID provided an analysis of

103 highly specific PPIs in cells[25], we used the AirID enzyme for proximity biotinylation of
104 antigens. To design an AirID-fusion antibody, the AGIA-tag system we developed
105 previously was utilised because the AGIA peptide tag (EEAAGIARP) is specifically
106 recognised by rabbit anti-AGIA mAb[28], and we had the gene sets for the construction and
107 production of its mAb. Proximity biotinylation prefers a short distance between the
108 antibody and antigen because it occurs within a very short range (~10 nm)[13]. To integrate
109 AirID with anti-AGIA mAb, we attempted to use two types of antibodies: 1)
110 AGIA-mAbID: AirID is fused to the C-terminus of the heavy chain in full-length IgG
111 antibody or 2) AGIA-FabID: AirID is fused to one of the fragments of antigen binding
112 instead of the Fc region (Fig. 1a). We considered the effect of the presence or absence of
113 the fragment crystallisable region (Fc region) on the biotinylation efficiency.

114 To obtain AGIA-mAbID and AGIA-FabID proteins, they were expressed in
115 Expi293F cells and purified by affinity chromatography using a nickel column (Fig. 1b)
116 because they have a 10x-histidine tag at their C-terminus. Biotinylation of these purified
117 proteins was mainly found in the heavy chain but not in each light chain (Fig. 1c). To check
118 the biotinylation ability of the antigen (Fig. 1d), the C-terminal region of human DRD1 was
119 used because the anti-AGIA mAb recognised it as the epitope[28]. Immunoblotting with an
120 anti-biotin antibody showed that antigen biotinylation by AGIA-FabID was higher than that
121 by AGIA-mAbID (arrowhead in Fig. 1e). AGIA-FabID also biotinylated other proteins

with an AGIA tag (Fig. 1f). Furthermore, to investigate whether AGIA-FabID could biotinylate a protein interacting with an antigen, an interaction between AGIA-tagged p53 and FLAG-GST-fusion MDM2 (FG-MDM2), previously used to check proximity biotinylation as a PPI model[24], was used (Fig. 1g). AGIA-FabID biotinylated both AGIA-p53 and FG-MDM2 (Fig. 1h) but did not biotinylate FLAG-p53 and FG-MDM2. Taken together, these results showed that FabID could biotinylate both antigens and their interacting proteins.

We previously showed that AirID functions in cells[24,25]. Since the pH conditions of the extracellular environment (pH ~7.4[29]) differ from those of the intracellular environment, we investigated the biotinylation activity of AGIA-FabID under various pH conditions. These results showed that AGIA-FabID has biotinylation activity between pH 7 and 8 (Supplementary Fig. 1a), suggesting that FabID can be used in this pH range, mimicking extracellular conditions.

Biotinylation of EGFR by EGFR-FabID or EGFR-mAbID

EGFR is a critical signalling mediator in many epithelial cancers[30]. EGFR consists of extracellular, transmembrane, and intracellular domains, with the C-terminal domain having tyrosine kinase activity. When a ligand such as EGF or TGF-α binds to EGFR, the structure of the extracellular domain of EGFR is altered, and EGFR forms a homodimer

141 with other EGFR or heterodimers with other ERBB family members. This dimerisation
142 activates the intracellular tyrosine kinase domain, which phosphorylates the tyrosine
143 residues in the C-terminal domain and transmits signals downstream[31]. In addition, EGFR
144 interacts with many membrane proteins[32,33]. However, it is often unclear whether these
145 interactions occur in the extracellular or intracellular regions of EGFR. Thus, we used
146 EGFR as a model membrane protein for proximity exPPI analysis. To make a proximity
147 biotinylation probe, we combined AirID and a previously reported anti-human EGFR
148 mouse mAb (no. 134) because it showed high affinity and selectivity for the extracellular
149 epitope (epitope region no. 377-386) of EGFR[34]. The EGFR-FabID and EGFR-mAbID
150 were constructed similarly to the anti-AGIA mAb shown in Fig. 1. Both EGFR-FabID and
151 EGFR-mAbID were purified and confirmed to make disulfide bonds on the Fab and IgG
152 (Fig. 2a). Full-length human EGFR was synthesised using a non-reducing wheat cell-free
153 protein production system because its extracellular region (25-645) has S-S bonds[35].
154 Biotinylation assays showed that full-length human EGFR was biotinylated *in vitro* by
155 EGFR-FabID and EGFR-mAbID (Fig. 2b) but not by negative controls, AGIA-FabID and
156 AGIA-mAbID.

157 In a method using an AirID-fused antibody, the accessibility of the AirID-antibody is
158 a very important factor for increasing the detection sensitivity. Many proximity
159 biotinylation methods use suspension cells[10] because antibodies can access the entire

surface area of suspension cells. Accordingly, Expi293F cells were used in suspension culture conditions and transfected with a plasmid containing the human EGFR gene (EGFR) or pcDNA3.1 empty plasmid (Mock). To validate the biotinylation ability of cells, EGFR-FabID or EGFR-mAbID was added to the medium and incubated with Expi293F cells transiently overexpressing EGFR for 2 h (Fig. 2c). Similar to the *in vitro* experiments above, both EGFR-FabID and EGFR-mAbID clearly biotinylated EGFR, whereas AGIA-FabID did not. A comparison of both probes indicated that the biotinylation efficiency of EGFR-FabID was much higher than that of EGFR-mAbID. The biotinylation of EGFR was also confirmed using a streptavidin-pull-down assay (STA-PDA in Fig. 2c). To understand why FabID was more highly biotinylated on cells than mAbID, we performed structural modelling of FabID and mAbID with the extracellular region of EGFR, as previously reported[35]. The modelling showed that the proximity distance between the extracellular domain and EGFR-FabID (Fig. 2d) or EGFR-mAbID (Fig. 2e) is 9.1 and 13.9 nm respectively, indicating that EGFR-FabID is less distant than EGFR-mAbID and thus may have greater biotinylation efficiency than EGFR-mAbID.

TurboID, another highly active biotinylation enzyme[22], was also fused with the same Fab against EGFR. The productivity of TurboID-fusion Fab was lower than AirID-based EGFR-FabID in Expi293F cells (IB: His in Supplementary Fig. 1b), whereas high biotinylated proteins were found in the culture medium expressing TurboID-based

179 EGFR-FabID (IB: Biotin). Purified TurboID-based EGFR-FabID also showed higher
180 biotinylation than AirID-based EGFR-FabID in the heavy chain fragment (Supplementary
181 Fig. 1c). Moreover, *in vitro* biotinylation activity of TurboID-based EGFR-FabID was
182 much lower than that of AirID-based EGFR-FabID (arrowhead in Supplementary Fig. 1d).
183 Although TurboID-based EGFR-FabID was attempted, we could not purify TurboID-fused
184 cells from the culture media of Expi293F cells. As shown in Figure 1, AirID-based
185 AGIA-FabID was purified and had high proximity biotinylation activity. Taken together,
186 these results suggest that AirID is suitable for fabricating Fab-fusion molecules.

187 Next, to confirm whether biotinylation by EGFR-FabID occurs in the extracellular
188 region, biotinylated peptides were purified by using Tamavidin 2-REV and analysed by
189 LC-MS/MS according to previous reports[36,37]. MS analysis indicated that EGFR-FabID
190 biotinylated five and seven lysine residues in the extracellular and intracellular regions of
191 EGFR, respectively (Fig. 2f). Furthermore, since the anti-EGFR antibody recognises an
192 epitope around Ser380 in the extracellular region[34] and the 3D structure of the extracellular
193 region of EGFR has been reported (PDB code: 1IVO)[35], we estimated the distance between
194 the binding site of EGFR-FabID and biotinylation sites. These five biotinylation sites in the
195 extracellular region were localised within 5 nm of the epitope (Fig. 2g). These interval
196 values seem reasonable because the biotinylation range of the BioID enzyme is presumably
197 ~10 nm[13], strongly suggesting that EGFR-FabID binds to the epitope and subsequently

198 biotinylates it. Taken together, these results indicated that EGFR-FabID functions as a
199 specific proximity biotinylation probe in the extracellular region.
200
201 **Proximity exPPI analysis of EGFR by EGFR-FabID on suspension culture Expi293F**
202 **cells overexpressing EGFR transiently**
203 As shown in Fig. 2, EGFR-FabID catalyzed extracellular biotinylation of EGFR by
204 incubation with a suspension of Expi293F cells transiently overexpressing EGFR. EGFR
205 reportedly interacts with other membrane proteins[32,33]. LC-MS/MS analysis to determine
206 the biotinylation of other proteins revealed that EGFR-FabID biotinylated 639 peptides in
207 transiently EGFR-overexpressing Expi293F cells (Fig. 3a). Further, when AGIA-FabID
208 was used as a negative control, 189 peptides were significantly biotinylated by
209 EGFR-FabID ($P < 0.05$ and EGFR-FabID/AGIA-FabID Ratios > 1 in Supplementary Table
210 1). Since our detection method using Tamavidin 2-REV could identify biotinylation sites on
211 proteins[36,37], we analysed whether the biotinylation sites were localised in the extracellular
212 regions using TMHMM (https://services.healthtech.dtu.dk/service.php?/TMHMM-2.0/)[38]
213 and Uniprot (https://uniprot.org) databases. Statistically predominant biotinylation sites of
214 64 peptides were found in the extracellular region (red dots in Fig. 3b), and the remaining
215 125 peptides were localised in intracellular or unknown cellular regions (black dots,
216 Supplementary Table 1).

Further analysis focused on the 22 proteins that were biotinylated in their extracellular region because EGFR-FabID recognised the extracellular epitope. Based on the IntAct database, which includes EGFR-interacting proteins (https://ebi.ac.uk/intact/)[39], 12 proteins were known to interact with EGFR (see black characters in Fig. 3c). Twelve out of 22 proteins (55%) showed high follow-up capability with recorded evidence, suggesting that the remaining 10 clones were also new interacting or proximal proteins (see blue characters in Fig. 3c). To compare the proximal exPPIs with the existing PPI database, these interactions were analysed using the Drug Target Excavator (DTX) (https://harrier.nagahama-i-bio.ac.jp/dtx/). This database depicts human protein/metabolite interaction pathways between a given pair of proteins. For DTX analysis, a direct protein-protein interaction pathway is presented as one edge. If a protein-protein interaction has two edges, the interaction is mediated by one another protein. These results showed that proximal exPPIs induced by EGFR-FabID were found within three edges (see the DTX edge in Fig. 3c). In addition, pathway analysis of the 22 proteins showed individual interactions with EGFR rather than multiple interactions, forming a large network (Fig. 3d). Taken together, these results indicate that EGFR-FabID provides a proximity interactome of extracellular regions between EGFR and other membrane proteins in transiently EGFR-overexpressing suspended cells.

Biotinylation analysis of endogenous EGFR by EGFR-FabID in human A431 cells

Next, we attempted to determine whether EGFR-FabID works on endogenous EGFR located on the surface of adherent cells. To select an adherent cell type, the protein level of endogenous EGFR and the reactivity of EGFR-FabID were investigated using immunoblotting and STA-PDA. The anti-EGFR (clone EMab-134) reacted with the EGFR protein in eight cell lines (Supplementary Fig. 1e). The expression level of EGFR protein was the highest in human squamous carcinoma epithelial cells (A431), whereas it was not detected in HEK293T and Expi293F cells. Comparison of EGFR expression indicated that EGFR protein expression in A431 cells was higher than that in stably EGFR-overexpressing Expi293F cells and similar to that in transiently EGFR-overexpressing Expi293F. To validate the performance of EGFR-FabID, we compared five cell lines with different EGFR expression levels: A431 (high), Expi293F-EGFR stable (middle), HeLaS3 (low), NCI-H1975 (low), and NCI-H226 (low) cells. Immunoblotting showed that EGFR biotinylation by EGFR-FabID was found in all lysates (red arrowheads in Fig. 4a); this was confirmed using STA-PDA. In addition, immunostaining indicated that EGFR-FabID biotinylated EGFR on the extracellular region of the cell membrane in A431 cells (Fig. 4b), whereas AGIA-FabID did not. These results suggest that EGFR-FabID biotinylates endogenous EGFR in cells at low and high expression levels.

Many researchers have used A431 cells for EGFR analysis because the EGFR gene has been cloned from this cell line[40]. In addition, EGFR-FabID clearly biotinylated the endogenous EGFR protein in A431 cells (Fig. 4b). Based on these results, further analysis of exPPI interactions using EGFR-FabID on adherent cells was focused on A431 cells. Next, we examined whether the addition of EGFR-FabID affected the EGFR ligand response using gefitinib. In A431 cells, after EGF ligand treatment with or without gefitinib, EGFR-FabID was supplied to the cells. Using the phospho-EGFR specific antibody, immunoblotting indicated that the kinase activity of EGFR dramatically increased by the treatment of EGF ligand in the presence of EGFR-FabID (Fig. 4c) and was completely inhibited by gefitinib treatment. These results showed that EGFR-FabID did not affect EGFR activity after treatment with the EGF ligand.

Considering these responses of EGFR in A431 cells, biotinylation of EGFR by EGFR-FabID was attempted under three conditions, with or without EGF ligand and with gefitinib treatment in the presence of EGF. Biotinylation of EGFR was analysed using LC-MS/MS, as shown in Figure 2. Interestingly, three biotinylated peptides on K454, K479, and K487 or K489 were found under all conditions, and the K489-biotinylated peptide increased on treatment with EGF ligand (red dots in Fig. 4d). Two biotinylated peptides on K479 and K487 or 489 increased on treating EGFR with gefitinib and EGF ligand (Fig. 4e), indicating that biotinylation sites changed in the presence or absence of EGF ligand or the

presence of a kinase inhibitor. These results suggest that K489 or K479 biotinylation could be a marker of EGF binding or gefitinib treatment of EGFR using EGFR-FabID, respectively.

As shown in Figure 2, biotinylation sites of EGFR from transiently EGFR-overexpressing Expi293F cells were analysed and compared with biotinylation sites on endogenous EGFR in A431 cells. In the extracellular region, almost the same pattern of biotinylation sites was observed (Supplementary Fig. 2a). Interestingly, the intracellular region of endogenous EGFR in A431 cells was not biotinylated by EGFR-FabID. However, in transiently EGFR-overexpressing Expi293F cells, the intracellular region was biotinylated at seven sites (black dots in Fig. 4c and Supplementary Fig. 2b), suggesting that transiently overexpressed EGFR proteins contain a mixture of forms that differ in conformation from endogenous EGFR proteins on the plasma membrane. Taken together, these results indicate that EGFR-FabID profiling of biotinylation sites on the extracellular region could help understand the various conformations of EGFR on the cell membrane.

Total proximity exPPI analysis using EGFR-FabID among three cell lines

The biotinylation sites of the EGFR protein were detectable in adherent A431 cells (Fig. 4). Therefore, to evaluate the potential versatility of EGFR-FabID in adherent cells and the commonality of proximity proteins of EGFR, the human lung squamous cell carcinoma cell

293 line NCI-H226 was also used for EGFR exPPI analysis as a new adherent cancer cell line.
294 Biotinylated proteins from A431 and NCI-H226 cells, with or without EGF ligand and with
295 gefitinib treatment in the presence of EGF, were analysed (Fig. 5a, Supplementary Table 2,
296 Supplementary Table 3). LC-MS/MS analysis revealed 481 and 849 biotinylated peptides
297 from A431 and NCI-H226 cells, respectively, under the three treatment conditions. The
298 biotinylation site in the intracellular region of EGFR was also not found in NCI-H226 cell
299 lines expressing endogenous EGFR (Supplementary Fig. 2a), similar to A431 cells. The
300 location of biotinylation sites was identified using TMHMM
301 (http://www.cbs.dtu.dk/services/TMHMM/) and Uniprot (https://uniprot.org) databases;
302 216 and 347 biotinylated peptides from A431 and NCI-H226 cells, respectively, were
303 annotated as peptides on the cell surface (red characters in Fig. 5a and red dots in Fig. 6a).
304 The remaining peptides were localised in intracellular or unknown cellular regions
305 (Supplementary Table 2, Supplementary Table 3). Finally, of these extracellular
306 biotinylated peptides, 44 and 66 proteins, including EGFR, were found to be membrane
307 proteins showing proximal exPPI with EGFR in A431 and NCI-H226 cells, respectively
308 (Supplementary Fig. 3a). The DTX analysis revealed 15 and 16 proteins from A431 and
309 NCI-H226 cells, respectively, interacting with EGFR. The remaining 29 and 50 proteins
310 from the A431 and NCI-H226 cells, respectively, were new proximal exPPI candidates
311 (denoted by blue numbers and protein names in Fig. 5a and Supplementary Fig. 3a).

312 Commonality analysis was performed based on the biotinylated protein data from the
313 three cell lines (EGFR-overexpressing Expi293F, A431, and NCI-H226). Except for EGFR,
314 five proteins: EEF1A1 (elongation factor 1-alpha 1), ENO1 (alpha-enolase), MICA (MHC
315 class I polypeptide-related sequence A), INSR (insulin receptor), and CD44 (cell
316 differentiation 44), were the most common proximal exPPI proteins, of which EEF1A1[33]
317 and ENO1[41] were known EGFR interactors (see black characters in Fig. 5b), and MICA,
318 INSR, and CD44 were new ones (see blue characters). In addition, 15 common proteins
319 were found between the A431 and NCI-H226 cell lines and consisted of 6 known and 9
320 novel proteins. Although Expi293F cells overexpressing EGFR are floating cells and the
321 remaining two cell lines, A431 and NCI-H226, are adherent cells, common proteins,
322 including known interactors, were found between each cell, indicating that EGFR-FabID
323 has similar functions in both adherent and non-adherent cells. The remaining 8, 19, and 41
324 proteins were independently observed in each cell line, suggesting that exPPIs with EGFR
325 may differ by cell type. The proximity exPPI results of the three cell lines with
326 EGFR-FabID revealed many known interacting proteins, suggesting that EGFR exPPI may
327 occur in complex with known interacting proteins.
328 To further compare the proximity exPPIs with the existing PPI database, these
329 interactions were analysed using DTX [https://harrier.nagahama-i-bio.ac.jp/dtx/)].
330 Interaction network diagrams of biotinylated proteins in A431 and NCI-H226 cells showed

that many proteins interacted with EGFR within three nodes (Fig. 5c). In A431 cells, all but DSG3 interacted with EGFR within two nodes. Some biotinylated proteins also interacted with each other. In NCI-H226 cells, all proteins, except L1CAM, interacted with EGFR within two nodes. The interaction network diagram, including proteins mediating interactions with EGFR, also confirmed that some biotinylated proteins mediate common molecules in the three cell lines (Supplementary Fig. 3b). Taken together, these results indicate that this approach using EGFR-FabID could be used to analyse the proximal extracellular interacting proteins of EGFR on the cell membranes of both adherent and floating cells.

Dynamic responses of proximity exPPIs on treatment with EGF ligand with or without gefitinib

In the EGF signalling response, dimeric EGFR phosphorylate each other at tyrosine residues in the intracellular region to form a signal complex. Gefitinib is a highly specific tyrosine kinase inhibitor of EGFR[27]. To understand the effect of gefitinib on exPPI, we compared the proximal exPPIs in A431 and NCI-H226 cells in the presence of EGF ligand (EGF) and EGF plus gefitinib (EGF+gefitinib) with a control without ligand (DMSO). From each treatment of the two cell lines, proximity exPPI analysis of EGFR yielded approximately 30 and 35-50 proteins, respectively (Fig. 6a, Supplementary Fig. 4). These

proximity exPPI proteins were analysed using a heatmap based on protein data from LC-MS/MS (Supplementary Table 4 and 5). In both A431 and NCI-H226 cells, 20 proteins were common proximity exPPIs (Fig. 6b)(HLA-C was removed from the common proteins because no values were detected in the protein MS data for A431 cells.), and the remaining 23 and 46 proteins were specific to A431 and NCI-H226 cells, respectively (Supplementary Fig. 5). Interestingly, EGFR-FabID-driven biotinylation was dramatically increased or decreased by EGF treatment compared with that by DMSO treatment. Furthermore, gefitinib treatment in the presence of EGF (EGF+gefitinib) also affected biotinylation of the proximal exPPIs with EGFR, suggesting that treatment with EGF ligands and tyrosine kinase inhibitors changes the proximity exPPIs of EGFR.

To confirm the presence of exPPIs with EGFR, we attempted to biochemically detect the interaction between the extracellular region of EGFR using the AlphaScreen method. PTK7 (tyrosine receptor kinase 7), INSR, and ADAM17 (disintegrin and metalloproteinase domain-containing protein 17), commonly found in proximity exPPIs with EGFR-FabID in both A431 and NCI-H226 cells, were selected. PTK7 and INSR share downstream signalling with EGFR[42,43,44], although they are not known as EGFR interactors. ADAM17 is also a major protease of the EGF family[45]. For the biochemical interaction of these proteins with the extracellular domain of EGFR, the extracellular region of EGFR was synthesised by a wheat cell-free system to form S-S complexes, and the extracellular

369 interactions were analysed using the AlphaScreen method. Since the alpha subunit of INSR
370 is known as the extracellular insulin-binding site[46], it was used in the assay. The
371 AlphaScreen method showed that PTK7, INSR alpha, and ADAM17 significantly bound to
372 the extracellular domain of EGFR (Fig. 6c). Furthermore, the interaction of PTK7 and
373 INSR with EGFR was also confirmed using the NanoBiT method, which allows the
374 measurement of interacting proteins in cultured cells (Fig. 6d). However, ADAM17 did not
375 work on the NanoBiT method.

376 Next, the change in proximity exPPIs in EGF, with or without gefitinib treatment,
377 was validated by ploximity ligation assay method (PLA) in A431 cells. As shown in Fig. 6b,
378 proximity exPPI of PTK7 with EGFR was reduced by gefitinib treatment. A large number
379 of PLA signals were detected in PTK7, and the PLA signal was also reduced by
380 EGF+gefitinib treatment compared with that by EGF treatment. (Fig. 6e). In contrast, the
381 proximity exPPI of INSR was increased by EGF and EGF+gefitinib (Fig. 6b), and the PLA
382 signal showed a significant increase (INSR in Fig. 6e). Furthermore, the proximity exPPI of
383 ADAM17 with EGFR also increased by EGR+gefitinib treatment, and the PLA signal also
384 increased in the EGF+gefitinib treatment (ADAM17 in Fig. 6e). These results indicated that
385 PLA signals were similar to biotinylation signals from EGFR-FabID proximity exPPIs with
386 EGFR. Taken together, these results strongly suggest that EGF ligand and a kinase inhibitor

provide dynamic exPPIs of EGFR on the cell membrane, and the FabID system can detect them via biotinylation.

Discussion

In this study, we used EGFR-FabID and EGFR-mAbID to study the exPPI of EGFR. The structural model suggested that the distance from FabID to the antigen was ~10 nm (Fig. 2d) and that from mAbID to the antigen would be ~14 nm (Fig. 2e), resulting in a higher biotinylation activity of EGFR-FabID than that of mAbID (Fig. 2c), although the *in vitro* biotinylation activity was almost the same (Fig. 2b). These results suggest that the distance between the probe and target protein is a key factor in proximity biotinylation of exPPI partners. Recently, EMARS[47,48] and μMap[10] were reported to detect proximal interactions with target membrane proteins. These methods used a full-size IgG antibody and not the Fab form. Furthermore, horseradish peroxidase (HRP) and a chemical molecule, ($\{Ir[dF(CF_3)ppy]_2(dtbbpy)\}PF_6$), are used as biotinylation catalysts in EMARS and μMap, respectively. Biotinylation via HRP with biotin phenol occurs in the range of 200-300 nm, while μMap has a biotinylation range of 50-100 nm[11]. In addition, the chemocatalytic molecule used in μMap is conjugated on a secondary antibody but not the primary antibody[10], suggesting that the distance between the biotinylation catalyst and target membrane protein is even further. FabID conjugates the AirID enzyme directly to the C-terminus of Fab. Taken together, the FabID system can efficiently biotinylate interacting proteins in the proximity of membrane proteins, thus making it the ideal method for the analysis of exPPIs on the cell membrane.

Using an EGFR-FabID system based on AirID to analyse exPPIs of the EGFR protein in living cell lines (both adherent and nonadherent cells), we revealed biotinylation sites by

411 LC-MS/MS using Tamavidin2-REV[36,37] and indicated that proximity biotinylation occurred
412 in the extracellular region. The analysis, therefore, provided proximity exPPIs with EGFR
413 and found many well-known EGFR interactors, as well as new proximity exPPI candidate
414 proteins (Fig. 5). Individual analyses also indicated direct exPPIs with the extracellular
415 region of EGFR (Fig. 6). Because other conventional methods have not identified
416 biotinylation sites, there is no information on the proximal region of the identified proteins.
417 These results indicate that biotinylation sites provide important information for interactome
418 analysis of membrane proteins.

419 The FabID system showed that exPPI with EGFR changes dynamically with the
420 addition of EGF ligand and gefitinib (Fig. 6 and Supplementary Fig. 5). EGF ligands
421 induce dimerisation of EGFR along with other conformational changes[35]. The
422 EGFR-FabID method detected a change in biotinylation sites on EGFR with or without
423 EGF (Fig. 4d-e, and Supplementary Fig. 3), contributing to the dynamic influence of
424 proximity exPPIs with EGFR on the cell membrane. As EGF induces conformational
425 changes in the extracellular region of EGFR, it is consistent that EGF affects the interaction
426 of exPPIs with EGFR. In addition, gefitinib inhibits tyrosine kinase activity, resulting in
427 complete loss of phospho-tyrosine sites[49]. Since phospho-tyrosine is used as a scaffold site
428 for the formation of the EGF signal complex[50], gefitinib may also inhibit its complex
429 formation. The results of EGF+gefitinib treatment in EGFR-FabID, therefore, suggest that
430 the inhibition of EGFR complex formation in the intracellular region affects the interaction
431 with extracellular regions of EGFR. Taken together, FabID provides a new tool for
432 extracellular interaction analysis, as it can capture not only the interaction analysis of
433 extracellular regions but also interacting proteins altered by ligands and drugs.

434 The EGFR-FabID method revealed direct interactions in the extracellular domain of
435 INSR and EGFR, which interact during intracellular signalling[43,44]. This finding may

indicate that extracellular signalling interactions occur between heterogeneous receptors on the membrane. Further, the exPPI analysis of various receptor tyrosine kinases using FabID on the cell membrane may provide new insights into signalling cooperation in the extracellular region. Furthermore, since they can change with drug treatment, FabID-based exPPIs may provide a new perspective on drug development for receptor tyrosine kinases.

In conclusion, the FabID system for the analysis of extracellular interactions can capture not only the interaction analysis of extracellular regions but also interacting proteins altered by ligands and drugs, thus delivering a powerful tool for the study of membrane proteins.

Materials and Methods

Reagents

Gefitinib (FUJIFILM Wako) was dissolved in DMSO (FUJIFILM Wako) at 2 mM and stored at -20°C as stock solutions. EGF (FUJIFILM Wako) was dissolved in phosphate-buffered saline (PBS) at 100 μg/mL and stored at -20°C as stock solutions. Streptavidin Sepharose High Performance (Cytiva) was stored at 4°C as stock solutions.

Plasmids

pcDNA3.1(+) and pcDNA3.4 vectors were purchased from Invitrogen/Thermo Fisher Scientific and RIKEN, respectively. The pEU vector for wheat cell-free protein synthesis was constructed in our laboratory as previously described[51]. pBiT1.1-C[TK/LgBiT] and pBiT2.1-C[TK/SmBiT] were purchased from Promega. pcDNA3.4-TEV-His, pEU-bls-MCS, and pEU-FLAG-MCS plasmids were constructed by polymerase chain

460 reaction (PCR) using the In-Fusion system (Takara Bio) or PCR and restriction enzymes.
461 AirID was was constructed in our laboratory, as previously described[24]. EGFR and MDM2
462 were purchased from the Kazusa Clone collection[52] using pEU-FLAG-GST-EGFR. PTK7,
463 OTULIN, ADAM17 and p53 were purchased from Mammalian Gene Collection (MGC).
464 The *SHB and LHB* gene was kindly provided by Prof. Y. Matsuura of the Osaka University
465 Center for Infectious Diseases Education and Research. The pEU-FLAG-GST-DRD1 CTD
466 was constructed in our laboratory, as previously described [28]. The restriction enzyme sites
467 were added to EGFR, EGFR extracellular domain, PTK7, OTULIN, SHBs and ADAM17
468 by PCR. The EGFR extracellular domain was cloned into pEU-MCS and pEU-bls-MCS.
469 EGFR was cloned into pcDNA3.1(+)-MCS and pBiT1.1-C[TK/LgBiT] plasmids. OTULIN
470 and SHBs were cloned into pEU-AGIA-MCS. PTK7 and INSR[28-758aa] were cloned into
471 pEU-FLAG-MCS. PTK7 and INSR was cloned into pBiT2.1[TK/SmBiT], respectively.
472 ADAM17 and LHBs were cloned into pEU-FLAG-MCS. MDM2, and p53 were cloned
473 into pEU-FLAG-GST or pEU-AGIA vectors using the Gateway cloning system (Thermo
474 Fisher Scientific). cDNAs for the anti-AGIA antibody light chains and EmAb-134 light
475 chain were cloned into the pcDNA3.4 expression vector using PCR and In-Fusion Reaction.
476 The anti-AGIA heavy chain Fab fragment or EmAb-134 heavy chain Fab fragment was
477 cloned into pcDNA3.4-TEV-His using the In-Fusion HD Cloning Kit (Takara Bio) together
478 with the AirID or TurboID fragment to generate pcDNA3.4-anti-AGIA Heavy
479 Fab-AirID-TEV-His and pcDNA3.4-EmAb-134 Heavy chain-AirID-TEV-His, respectively.
480
481 **Cell culture and transfection**
482 Expi293F cells (Gibco/Thermo Fisher Scientific) were shaken at 125 ± 5 rpm at 37°C
483 under 8% CO_2 in Expi293F medium (Gibco/Thermo Fisher Scientific) supplemented with
484 100 U/mL penicillin and 100 μg/mL streptomycin (Gibco/Thermo Fisher Scientific). A431

(JCRB Cell Bank) cells were cultured in high-glucose DMEM (FUJIFILM Wako) supplemented with 10% fetal bovine serum (FBS; FUJIFILM Wako), 100 U/mL penicillin, and 100 μg/mL streptomycin (Gibco/Thermo Fisher Scientific) at 37°C under 5% CO_2. HeLa-S3 cells (JCRB Cell Bank) were shaken at 125 ± 5 rpm at 37°C under 8% CO_2 in Ham's F-12 (FUJIFILM Wako) supplemented with 100 U/mL penicillin and 100 μg/mL streptomycin (Gibco/Thermo Fisher Scientific). NCI-H1975 (ATCC) and NCI-H226 (ATCC) were cultured in RPMI160 GlutaMAX medium (Gibco/Thermo Fisher Scientific) supplemented with 10% fetal bovine serum (FUJIFILM Wako), 100 U/mL penicillin, and 100 μg/mL streptomycin (Gibco/Thermo Fisher Scientific) at 37°C under 5% CO_2. Expi293F cells were transiently transfected using Expi Fectamine 293 transfection kit (Gibco/Thermo Fisher Scientific).

Antibodies

The following horseradish peroxidase (HRP)-conjugated antibodies were used in this study: anti-FLAG (Sigma-Aldrich, A8592, 1:5000), anti-AGIA (produced in our laboratory, 1:10000)[28], anti-tubulin (MBL, PM054-7, 1:5000), anti-His (Santa Cruz, sc-8036, 1:1000), and biotin (Cell Signalling Technology, #7075, 1:1000). The following primary antibodies were used: anti-EGFR (clone EMab-134; produced in our laboratory, 1:1000)[34], anti-ADAM17 (Cell Signalling Technology, #3976, 1:1000), anti-P-EGFR-Tyr1173 (Cell Signalling Technology, #4407, 1:1000), anti-biotin (Cell Signalling Technology, #5597, 1:1000), anti-insulin receptor alpha (Cell Signalling Technology, #74118, 1:1000), anti-STAT3 (Cell Signalling Technology, #9132, 1:1000), anti-P-STAT3-Y705 (Cell Signalling Technology, #9145, 1:1000), and anti-PTK7 (proteintech, 17799-1-AP, 1:1000). Anti-rabbit IgG (HRP-conjugated, Cell Signalling Technology, #7074, 1:10000), anti-mouse IgG (HRP-conjugated, Cell Signalling Technology, #7076, 1:10000),

F(ab')2-Goat anti-Rabbit IgG (H+L) Cross-Adsorbed Secondary Antibody, Alexa Fluor 555 (Thermo Fisher Scientific, A21431), and goat anti-mouse IgG (H+L) Cross-Adsorbed Secondary Antibody, Alexa Fluor™ 488 (Thermo Fisher Scientific, A11001) were used as secondary antibodies.

Preparation of FabID and mAbID

FabID and mAbID were expressed using the Expi293F Expression System (Thermo Fisher Scientific), according to the manufacturer's instructions. The culture medium was purified using protein Ni Sepharose Excel (GE Healthcare). The supernatants were added to Ni Sepharose Excel (GE Healthcare) and incubated for 3 h at 4°C. The mixture was then washed with three-column volumes of wash buffer (20 mM sodium phosphate, 300 mM NaCl, and 10 mM imidazole). Proteins were eluted in 500 μL fractions with elution buffer (20 mM sodium phosphate, 300 mM NaCl, and 500 mM imidazole). The fractions were dialysed against PBS. Purified FabID and mAbID were frozen and stored at -80°C.

Immunoblot analysis

Protein samples were separated using SDS-PAGE and transferred onto polyvinylidene difluoride (PVDF) membranes (Millipore). The membranes were blocked using 5% skimmed milk (Megmilk Snow Brand) in TBST (20 mM Tris-HCl [pH 7.5], 150 mM NaCl, and 0.05% Tween20) at 27℃ for 1 h and then treated with the appropriate antibodies. Immobilon (Merck), ImmunoStar LD (FUJIFILM Wako), or EzWestLumi plus (Atto) were used as substrates for HRP, and the luminescence signal was detected using an ImageQuant LAS 4000 mini (GE Healthcare). In some blots, the membrane was stripped with a stripping solution (FUJIFILM Wako) and reprobed with other antibodies.

Wheat cell-free protein synthesis

The recombinant protein was synthesised using a wheat cell-free system. *In vitro* transcription and wheat cell-free protein synthesis were performed using the WEPRO1240 Expression Kit (Cell-Free Sciences) or Disulfide Bond PLUS Expression Kit (Cell-free Sciences). Transcription was performed using SP6 RNA polymerase, with plasmids or DNA fragments as templates. The translation reaction was performed in bilayer mode using the WEPRO1240 expression kit (Cell-Free Sciences) or Disulfide Bond PLUS Expression Kit (Cell-Free Sciences), according to the manufacturer's protocol. For biotin labelling of the bls-EGFR extracellular domain, cell-free synthesised crude biotin ligase (BirA) produced using the wheat cell-free expression system was added to the bottom layer, and 0.5 μM (final concentration) of d-biotin (Nacalai Tesque) was added to both the upper and lower layers, as described previously[8].

***In vitro* biotinylation assay with FabID and mAbID**

Wheat cell-free expression system synthesised each proteins were mixed with FabID or mAbID (Fin 80 ng/μL), added to the reaction mixture, and incubated for 1 h at 26°C. Next, d-biotin (Nacalai Tesque) was added at a concentration of 500 nM and incubated at 26°C for 3 h. After the reaction, biotinylated proteins were analysed using SDS-PAGE and immunoblotting.

Biotinylation of the protein complex by AGIA-FabID

Wheat cell-free expression system synthesised eath proteins were mixed and incubated for 1 h at 26°C. In addition, AGIA-FabID (Fin 80 ng/μL) was added to the reaction mixture and incubated for 1 h at 26°C. Next, d-biotin (Nacalai Tesque) was added at a concentration of 500 nM and incubated at 26°C for 5 h. After the reaction, biotinylated proteins were

560 analysed using SDS-PAGE and immunoblotting.

561

562 **AGIA-FabID pH resistance analysis**

563 One hundred microlitres of protein synthesised using the wheat cell-free protein synthesis
564 system was dialysed in 10 mL of buffer at each pH (100 mM HEPES-NaOH buffer pH =
565 7.0, 7.2, 7.4, 7.6, and 7.8; 200 mM Tris-HCl buffer pH = 8.0). After 24 h of dialysis, an *in*
566 *vitro* biotinylation assay was performed.

567

568 **Molecular docking of EGFR-FabID and EGFR-mAbID with EGFR extracellular**
569 **domains**

570 The complex model of EGFR-FabID and EGFR-mAbID was predicted using AlphaFold2
571 (AF2)[53]. The predictive antigen-binding region of EGFR-FabID was manually adjusted to
572 dock into epitope regions of the EGFR extracellular domains (Protein Data Bank (PDB)
573 code: 1IVO). The light and heavy chains of EGFR-FabID were superimposed onto the
574 structure of the anti-canine lymphoma monoclonal antibody (Mab231 and PDB code:
575 1IGT), and the predictive antigen-binding region of EGFR-mAbID was also manually
576 docked into epitope regions of EGFR extracellular domains (PDB code: 1IVO). All the
577 molecular structures were generated using PyMOL (Schrödinger).

578

579 **Stable cell line**

580 EGFR-overexpressing Expi293F cells were transfected with pcDNA3.1-EGFR in Expi293F
581 cells (5×10^6 cells). After 24 h of infection, the culture medium was exchanged, and 1
582 mg/mL Geneticin G418 (Sigma Aldrich) selection was started 24 h after exchanging the
583 culture medium.

584

Cell biotinylation assay with FabID

Biotinylation of EGFR on the plasma membrane was performed using EGFR-overexpressing Expi293F cells transfected with pcDNA3.1-EGFR. Expi293F cells (5×10^6 cells) were transfected with pcDNA3.1-EGFR (2μg) and incubated for 24 h. Next, 385 μL Expi293F medium (10 mM HEPES) and 115 μL FabID suspension cells reaction buffer [355.5 μg/mL EGFR-FabID, 22.2 mM ATP, 66.7 mM $MgCl_2$, and 333.3 μM d-biotin] were added and incubated at 37°C for 2 h with rotation. Cells were collected by centrifugation and washed twice with 1 mL of PBS. Cells were lysed with 500 μL RIPA buffer + protease inhibitor (Sigma-Aldrich), followed by sonication and streptavidin pull-down assays.

EGFR-stable (1.0×10^7 cells) and HeLa S3 cells (5×10^6 cells) were resuspended in 385 μL Expi293F medium (+10 mM HEPES) or D-MEM (FBS-,10 mM HEPES). Next, 115 μL FabID suspend cell reaction buffer was added and incubated at 37 °C for 2 h with rotation. Cells were collected by centrifugation and washed twice with 1 mL of PBS. Cells were lysed with 500 μL RIPA buffer + protease inhibitor (Sigma-Aldrich), followed by sonication and streptavidin pull-down assays.

For A431, NCI-H226, and NCI-H1975 cells, a 10 cm confluent dish was washed once with 2 mL PBS, after which 4.2 mL of D-MEM (FBS-, 10 mM HEPES), 800 μL FabID adherent cells reaction buffer (177.8 μg/mL EGFR-FabID, 22.2 mM ATP, 66.7 mM $MgCl_2$, and 333.3 μM d-biotin) were added and incubated at 37°C for 2 or 6 h. After the reaction, the cells were washed with PBS (2.5 mL) and dissolved in 500 μL of RIPA buffer + protease inhibitor (Sigma-Aldrich). After sonication, streptavidin pull-down assays were performed.

Streptavidin pull-down assay (STA-PDA) using suspension or adherent cells

Streptavidin Sepharose (20 µL/L sample) was washed three times in wash buffer (50 mM Tris-HCl pH 7.5, 100 mM NaCl, 1% SDS), resuspended in 200 µL of wash buffer, and added to the sample. The mixture was then rotated at room temperature for 1 h, and the supernatant was removed by centrifugation. Streptavidin Sepharose was washed three times with 1 mL of wash buffer and boiled in 2× sample buffer (40 µL) at 100°C for 10 min. The supernatant was recovered by centrifugation.

Kinase assay using A431 cells

A431 (3.0×10^6 cells/mL) cells were seeded in 24-well plates. After 24 h, the cells media was replaced with serum-free media, and cells were treated with DMSO (final 0.1%) or 2 µM gefitinib for 2 h. Next, EGF (100 ng/mL) was added for 5 min, and cells were treated with 80 ng/µL EGFR-FabID. After 15 min, the cells were collected and lysed in 100 µL of 2× sample buffer + 10% mercaptoethanol. Phosphorylation of EGFR and STAT3 activated by EGF stimulation was confirmed by western blotting using specific antibodies.

Preparation of cell lysates treated with EGFR-FabID for the enrichment of biotinylated peptides

Biotinylation of EGFR on the plasma membrane using EGFR-overexpressing Expi293F cells transfected with pcDNA3.1-EGFR was assessed in three biological replicates. Expi293F cells (5×10^6 cells) were incubated with EGFR overexpression for 24 h. Next, 385 µL Expi293F medium (10 mM HEPES) and 115 µL FabID suspend cell reaction buffer were added and incubated at 37°C for 2 h with rotation. Cells were collected by centrifugation and washed twice with 1 mL HEPES-Saline (20 mM HEPES-NaOH, pH 7.5, 137 mM NaCl). The cells were then lysed in 500 µL Gdm-TCEP buffer (6 M guanidine-HCl, 100 mM HEPES-NaOH pH 7.5, 10 mM TCEP, and 40 mM

chloroacetamide).

A 10 cm dish confluent with A431 cells in three biological replicates was washed once with 1 mL PBS. Then, 2.1 mL of D-MEM (FBS-) was added, and cells were treated with DMSO or 2 μM gefitinib (DMSO final 0.1%) for 2 h, followed by treatment with 100 ng/mL EGF. Next, 800 μL FabID adherent cell reaction buffer was added to the medium and incubated at 37°C for 2 h. After the reaction, cells were washed with 5 mL Hepes-Saline (20 mM HEPES-NaOH, pH 7.5, 137 mM NaCl) and lysed in 500 μL Gdm-TCEP buffer (6 M guanidine-HCl, 100 mM HEPES-NaOH pH 7.5, 10 mM TCEP, and 40 mM chloroacetamide). The lysates were then grouped into three tubes of 500 μL each, with one in each treatment section.

Confluent NCI-H226 cells (10 cm dish, five biological replicates) were washed once with 1 mL PBS. Then, 2.1 mL of D-MEM (FBS-) was added, and cells were treated with DMSO or 2 μM gefitinib (DMSO final 0.1%) for 1 h, followed by treatment with 5 μL EGF (100 μg/μL). Next, 800 μL FabID adherent cell reaction buffer was added to the medium and incubated at 37°C for 3 h. After the reaction, cells were washed with 5 mL Hepes-Saline (20 mM HEPES-NaOH, pH 7.5, 137 mM NaCl) and lysed in 300 μL Gdm-TCEP buffer (6 M guanidine-HCl, 100 mM HEPES-NaOH pH 7.5, 10 mM TCEP, and 40 mM chloroacetamide). The lysates were then grouped into three tubes of 500 μL each, with one in each treatment section.

Enrichment of biotinylated peptides using Tamavidin 2-REV

The cell lysates in Gdm-TCEP buffer were dissolved by heating and sonication and then centrifuged at 20,000 × *g* for 15 min at 4°C. The supernatants were recovered, and proteins were purified by methanol–chloroform precipitation and solubilised using PTS buffer (12 mM SDC, 12 mM SLS, 100 mM Tris-HCl, pH8.0). After sonication and heating, the

protein solution was diluted 5-fold with 100 mM Tris-HCl, pH8.0 and digested with trypsin (MS grade, Thermo Fisher Scientific) at 37°C overnight. The resulting peptide solutions were diluted 5-fold with TBS (50 mM Tris-HCl, pH 7.5, 150 mM NaCl). Biotinylated peptides were captured on a 15 µL slurry of MagCapture HP Tamavidin 2-REV magnetic beads (FUJIFILM Wako) after incubation for 3 h at 4°C. After washing with TBS five times, the biotinylated peptides were eluted with 100 µL of 1 mM biotin in TBS for 15 min at 37°C twice. The combined eluates were desalted using GL-Tip SDB (GL Sciences), evaporated in a SpeedVac concentrator (Thermo Fisher Scientific), and re-dissolved in 0.1% TFA and 3% acetonitrile (ACN).

Data-dependent LC-MS/MS analysis

LC-MS/MS analysis of the resultant peptides was performed on an EASY-nLC 1200 UHPLC connected to an Orbitrap Fusion mass spectrometer using a nanoelectrospray ion source (Thermo Fisher Scientific). The peptides were separated on a 150-mm C_{18} reversed-phase column with an inner diameter of 75 µm (Nikkyo Technos) using a linear 4–32% ACN gradient for 0–60 min, followed by an increase to 80% ACN for 10 min. The mass spectrometer was operated in data-dependent acquisition mode with a maximum duty cycle of 3 s. The MS1 spectra were measured with a resolution of 120,000, an automatic gain control (AGC) target of 4×10^5, and a mass range of 375–1,500 *m/z*. HCD MS/MS spectra were acquired in a linear ion trap with an AGC target of 1×10^4, an isolation window of 1.6 *m/z*, a maximum injection time of 200 ms, and a normalised collision energy of 30. Dynamic exclusion was set to 10 s. Raw data were directly analysed against the Swiss-Prot database restricted to *Homo sapiens* using Proteome Discoverer version 2.4 (Thermo Fisher Scientific) with the Sequest HT search engine. The search parameters were as follows: (a) trypsin as an enzyme with up to two missed cleavages, (b) precursor mass

tolerance of 10 ppm, (c) fragment mass tolerance of 0.6 Da; (d) carbamidomethylation of cysteine as a fixed modification, and (e) acetylation of protein N-terminus, oxidation of methionine, and biotinylation of lysine as variable modifications. Peptides were filtered at a false discovery rate (FDR) of 1% using the Percolator node. Label-free quantification was performed based on the intensities of the precursor ions using a precursor ion quantifier node. Normalisation was performed such that the total sum of the abundance values for each sample over all peptides was the same. For statistical analyses of the MS data, the *P*-values in each volcano plot were calculated using Student's *t*-tests. The adjusted *P*-values were calculated by controlling the FDR and are shown in the Supplementary table.

AlphaScreen-based biochemical assays using recombinant proteins

The bls-EGFR extracellular domain and FLAG fusion proteins were synthesised using a Disulfide Bond PLUS Expression Kit (CellFree Science). Proteins synthesized using the wheat cell-free expression system were mixed in 15 μL of reaction buffer (100 mM Tris-HCl pH 8.0, 1 mg/mL BSA, 100 mM NaCl, and 0.1% Tween20) and incubated at 26°C for 1 h. Then, 10 μL of the detection mixture containing 0.1 μL protein A acceptor beads and 0.1 μL streptavidin donor beads (PerkinElmer) in the reaction buffer were mixed. After incubation at 26°C for 1 h, the luminescence signal was detected using an Envision microplate reader (PerkinElmer).

Immunofluorescent staining

The cells were fixed with 4% paraformaldehyde in phosphate-buffered saline (PBS) for 15 min at room temperature. Cells were incubated with anti-EGFR (clone EMab-134), anti-biotin, and 4',6-diamidino-2-phenylindole (DAPI) overnight at 4°C after blocking with 0.5% CS in TBST overnight. After washing with TBST, the cells were incubated with the

appropriate Alexa Fluor 488 or 555 conjugated secondary antibody for 1 h at room temperature. After washing with TBST, the coverslips were mounted with anti-fade (Invitrogen/Thermo Fisher Scientific) and observed under a BZ-X810 Microscope (Keyence).

NanoBiT PPI assay

Plasmids (25 ng of pBiT2.1-PTK7-SmBiT or pBiT2.1-INSR-SmBiT together with 25 ng of pBiT1.1-DHFR-LgBiT or pBiT1.1-EGFR-LgBitT) and 50 ng of pcDNA3.1-(+) vectors were transfected into HEK293T cells in 96 well-plate using polyethyleneimine (PEI) Max (MW 40,000) (PolyScience, Inc.) After 24 h, the culture medium was replaced with 80 µL Opti-MEM reduced serum medium (Gibco). Then, 20 µL Nano-Glo Live Cell Reagent (Promega) was added and measured NanoBiT signal using the GloMAX Discover System (Promega).

Proximity ligation assay

A431 cells were cultured on 13 mm poly L-lysine-coated glass slides (Matsunami) in 24-well plates. After culturing for 24 h, the cells were washed two times with PBS. Cells were fixed with 4% paraformaldehyde in PBS for 15 min at room temperature and permeabilised with 0.1% Triton X-100 in PBS (PTK7 and ADAM17); INSR was not amenable to permeabilisation. The cells were then washed twice with PBS and blocked with Duolink block solution for 1 h at 37 ℃. Next, the cells were stained overnight at 4°C with primary antibodies diluted in Duolink antibody dilution buffer. Then, the cells were washed twice with wash buffer A (10 mM Tris, pH-7.4, 150 mM NaCl, and 0.05% Tween) and incubated with 20 µL of secondary antibody (4 µL anti-mouse PLUS antibody + 4 µL anti-rabbit MINUS antibody + 12 µL Duolink® dilution buffer) at 37°C for 1 h. The

735 secondary antibody mix was gently aspirated and washed twice with wash buffer A. Fifteen
736 microliters of ligation mix was added to each sample and incubated at 37°C for 30 min.
737 Slides were washed twice with wash buffer A for 2 min each. Fifteen microliters of the
738 polymerase mix was added to each sample and incubated for 100 min at 37°C. The
739 amplification mix was aspirated and washed twice with wash buffer B (200 mM Tris,
740 pH-7.5, 100 mM NaCl) for 10 min each. The slides were washed once with 0.01× buffer B
741 for 1 min. After aspirating buffer B, slides were then mounted using Duolink® in situ
742 mounting medium with DAPI (Sigma-Aldrich). PLA foci and the number of nuclei were
743 measured using Andy's PLA algorithm (biological replicate, n=9)[54]. A table of the
744 optimised image parameters used for the PLA image analysis is provided in the source data.
745
746 **Bioinformatics analyses**
747 Proteins predominantly biotinylated were identified using EGFR-FabID. To determine the
748 subcellular localisation of the biotinylated proteins, the TMHMM
749 (https://services.healthtech.dtu.dk/service.php?TMHMM-2.0) software and the UniProt
750 database were employed. If a protein has transmembrane helices or is annotated as
751 membrane localised, it was considered as a membrane located protein. If the biotinylation
752 site of the membrane located protein was predicted as extracellular region, it was
753 considered to be located on extracellular region. The known protein-protein interaction data
754 were downloaded from the IntAct database (https://www.ebi.ac.uk/intact). Pathway
755 diagrams of protein-protein interaction network based on data analysed by DTX
756 (https://harrier.nagahama-i-bio.ac.jp/dtx/) were generated using the Cytoscape software
757 (https://cytoscape.org).
758
759 **Statistical analyses**

Significant changes were analysed by Student's t-tests using Microsoft Excel spreadsheets with a basic statistical program or one-way ANOVA followed by Tukey's post-hoc test using GraphPad Prism 9 software (GraphPad, Inc.). For all tests, $P < 0.05$ was considered statistically significant. Immunoblot analyses and streptavidin pull-down assays were repeated more than twice, with similar results.

Data availability

The MS proteomics data have been provided in Supplementary Table 1–5 and deposited to the ProteomeXchange Consortium via the jPOST partner repository with the dataset identifiers PXD039449 (https://repository.jpostdb.org/preview/19410604663c3ad3416706, Access key: 2160) (Proximity biotinylation of Expi293F cells overexpressing EGFR by EGFR-FabID), PXD039450 (https://repository.jpostdb.org/preview/181042815963c3b3fcc72e4, Access key: 4562) (Proximity biotinylation of A431 cells by EGFR-FabID), and PXD039451 (https://repository.jpostdb.org/preview/209858974363c3b7e2bc17c, Access key: 3354) (Proximity biotinylation of NCI-H226 cells by EGFR-FabID).

Acknowledgements

We thank Prof. Y. Matsuura (Osaka University) for providing *LHB* and *SHB* genes. We would like to thank the Applied Protein Research Laboratory of Ehime University. This work was partially supported by the Platform Project for Supporting Drug Discovery and Life Science Research [Basis for Supporting Innovative Drug Discovery and Life Science Research (BINDS)] from the Japan Agency for Medical Research and Development (AMED) under Grant Number JP21am0101077 (T.S.), 22ama121010j0001 (T.S.), JP22ama121008 (Y.K.). This work was also partially supported by JSPS KAKENHI (19H03218 and JP21K19230 for T.S.), Joint Usage and Joint Research Programs of the Institute of Advanced Medical Sciences, Tokushima University (H.K., T.S.), and Takeda Science Foundation.

Author contributions

K.Y. performed cloning and characterisation of AGIA-mAbID, EGFR-mAbID and EGFR-FabID, cell-based assays, and biotinylation assay; R.S. performed cloning and analysis of AGIA-FabID; K.N. and H.K. performed enrichment of biotinylated peptides and LC-MS/MS analyses; H.F. performed structural modelling; M.K.K. and Y.K. cloned antibodies; A.H. and T.S. performed bioinformatic analyses of biotinylated sites and proteins; K.Y. and T.S. analysed the data and wrote the draft paper; T.S. conceived the research and designed the study; H.K. and T.S. designed the experiments, wrote the paper, and all authors revised the manuscript.

797

798 **Competing interests**

799 The authors declare no competing interests.

800

801 **Corresponding authors**

802 Correspondence and requests for materials should be addressed to Tatsuya Sawasaki

803 (sawasaki@ehime-u.ac.jp) and Hidetaka Kosako (kosako@tokushima-u.ac.jp).

804

References

1. Bechtel TJ, et al., Strategies for monitoring cell–cell interactions. *Nat Chem Biol*. **17,** 641-652 (2021).
2. Bausch-Fluck D, et al., The in silico human surfaceome. *Proc Natl Acad Sci USA*. **115,** E10988-E10997 (2018).
3. Yin, H. & Flynn, A.D., Drugging Membrane Protein Interactions. *Annu Rev Biomed Eng*. **18,** 51-76 (2016).
4. Zhao, S. et al., Screening and identification of host proteins interacting with Theileria annulata cysteine proteinase (TaCP) by yeast-two-hybrid system. *Parasite Vectors*. **10**, 536 (2017).
5. Li, J. et al., Development of a membrane-anchored ligand and receptor yeast two-hybrid system for ligand-receptor interaction identification. *Sci. Rep.* **6**, 35631 (2016).
6. Ohshiro, K. et al. Identification of a novel estrogen receptor-alpha variant and its upstream splicing regulator. *Mol. Endocrinol.* **24**, 914–922 (2010).
7. Han, J. et al., The identification of novel protein-protein interactions in liver that affect glucagon receptor activity. *PLoS ONE*. **10**, e0129226 (2015).
8. Nemoto, K. et al., Tyrosine phosphorylation of the GARU E3 ubiquitin ligase promotes gibberellin signalling by preventing GID1 degradation. *Nat. Commun.* **8**, 1004 (2017).
9. Takahashi, H. et al., Establishment of a wheat cell-free synthesized protein array containing 250 human and mouse e3 ubiquitin ligases to identify novel interaction between e3 ligases and substrate proteins. *PLoS ONE.* **11**, e0156718 (2016).
10. Geri, J.B. et al., Microenvironment mapping via Dexter energy transfer on immune cells. *Science.* **367,** 1091-1097 (2020).
11. Oakley, J.V. et al., Radius measurement via super-resolution microscopy enables the development of a variable radii proximity labeling platform. *Proc Natl Acad Sci USA.* **119**, e2203027119 (2022).
12. Bosch JA, Chen CL, Perrimon N., Proximity-dependent labeling methods for proteomic profiling in living cells: An update. *Wiley interdiscip Rev Dev Biol*. **10**(1):e392 (2020).
13. Kim, D.I. et al., Probing nuclear pore complex architecture with proximity-dependent biotinylation. *Proc. Natl. Acad. Sci. USA.* **111**, 2453–2461 (2014).
14. Go, C.D. et al., A proximity-dependent biotinylation map of a human cell. *Nature.* **595**, 120-124 (2021).
15. Varnaitė, R. & MacNeill, S.A., Meet the neighbors: Mapping local protein interactomes by proximity-dependent labeling with BioID. *Proteomics*. **16,** 2503-2518 (2016).
16. Samavarchi-Tehrani P., Samson, R., Gingras. A.C., Proximity Dependent Biotinylation: Key Enzymes and Adaptation to Proteomics Approaches. *Mol Cell Proteomics.* **19,** 757-773 (2020).

17. Ge, Y. et al., Enzyme-Mediated Intercellular Proximity Labeling for Detecting Cell-Cell Interactions. *J Am Chem Soc*. **141,** 1833-1837 (2019).
18. Liu, Q. et al., A proximity-tagging system to identify membrane protein-protein interactions. *Nat Methods.* **15,** 715-722 (2018).
19. Martell, J.D. et al., Engineered ascorbate peroxidase as a genetically encoded reporter for electron microscopy. *Nat. Biotechnol*. **30**, 1143–1148 (2012).
20. James, C. et al., Proteomic mapping by rapamycin-dependent targeting of APEX2 identifies binding partners of VAPB at the inner nuclear membrane. *J Biol Chem.* **294,** 16241–16254 (2019).
21. Choi-Rhee, E., Schulman, H., Cronan, J.E. Promiscuous protein biotinylation by Escherichia coli biotin protein ligase. *Protein Sci.* **13,** 3043–3050 (2004).
22. Branon, T.C. et al. Efficient proximity labeling in living cells and organisms with TurboID. *Nat Biotechnol.* **36**, 880-887 (2018).
23. Roux, K.J. et al., A promiscuous biotin ligase fusion protein identifies proximal and interacting proteins in mammalian cells. *J Cell Biol*. **196,** 801-10 (2012).
24. Kido, K. et al., AirID, a novel proximity biotinylation enzyme, for analysis of protein–protein interactions. *eLife.* **9**, e54983 (2020).
25. Yamanaka, S. et al., A proximity biotinylation-based approach to identify protein-E3 ligase interactions induced by PROTACs and molecular glues. *Nat. Commun*. **13**, 183 (2022).
26. Shafraz, O. et al., Mapping transmembrane binding partners for E-cadherin ectodomains. *Proc Natl Acad Sci USA.* **117,** 31157-31165 (2020).
27. Dhillon, S. Gefitinib: a review of its use in adults with advanced non-small cell lung cancer. *Targeted Oncol.* **10**, 153–170 (2015).
28. Yano, T. et al., AGIA tag system based on a high affinity rabbit monoclonal antibody against human dopamine receptor D1 for protein analysis. *PLoS ONE*. **11**, e0156716 (2016).
29. Gerweck, L.E. & Seetharaman, K., Cellular pH gradient in tumor versus normal tissue: Potential exploitation for the treatment of cancer. *Cancer Res*. **56**, 1194–1198 (1996).
30. Talukdar, S. et al., EGFR: An essential receptor tyrosine kinase-regulator of cancer stem cells. *Adv Cancer Res*. **147,** 161-188 (2020).
31. Freed, D.M. et al., EGFR Ligands Differentially Stabilize Receptor Dimers to Specify Signaling Kinetics. *Cell*. **171,** 683-695.e18 (2017).
32. Foerster, S. et al., Characterization of the EGFR interactome reveals associated protein complex networks and intracellular receptor dynamics. *Proteomics*. **13**, 3131–3144 (2013).

878 33. Thelemann, A. et al., Phosphotyrosine Signaling Networks in Epidermal Growth Factor
879 Receptor Overexpressing Squamous Carcinoma Cells. *Mol Cell Proteomics.* **4,** 356-76
880 (2005).
881 34. Kaneko, M.K. et al., Elucidation of the critical epitope of an anti-EGFR monoclonal
882 antibody EMab-134. *Biochem Biophys Rep.* **14,** 54-57 (2018).
883 35. Ogiso, H. et al., Crystal Structure of the Complex of Human Epidermal Growth Factor
884 and Receptor Extracellular Domains. *Cell*. **110,** 775-87 (2002).
885 36. Motani, K. & Kosako, H., Activation of stimulator of interferon genes (STING) induces
886 ADAM17-mediated shedding of the immune semaphorin SEMA4D. *J Biol Chem*. **293,**
887 7717–7726 (2018).
888 37. Nishino, K. et al., Optimized Workflow for Enrichment and Identification of
889 Biotinylated Peptides Using Tamavidin 2-REV for BioID and Cell Surface Proteomics.
890 *J Proteome Res*. **21**, 2094-2103 (2022).
891 38. Krogh, A. et al., Predicting transmembrane protein topology with a hidden Markov
892 model: application to complete genomes. *J Mol Biol*. **305,** 567-80 (2001).
893 39. Hermjakob, H. et al., IntAct: an open source molecular interaction database. *Nucleic*
894 *Acids Res*. 32:D452-D455 (2004).
895 40. Carpenter, G., King, L., Cohen, S., Epidermal growth factor stimulates phosphorylation
896 in membrane preparations in vitro. *Nature*. **276,** 409-10 (1978).
897 41. Hua, Q. et al., AL355338 acts as an oncogenic lncRNA by interacting with protein
898 ENO1 to regulate EGFR/AKT pathway in NSCLC. *Cancer Cell Int*. **21,** 525 (2021).
899 42. Cui, N.P. et al., Protein Tyrosine Kinase 7 Regulates EGFR/Akt Signaling Pathway and
900 Correlates With Malignant Progression in Triple-Negative Breast Cancer. *Front Oncol*.
901 **11,** 699889 (2021).
902 43. Stefani, C. et al., Growth Factors, PI3K/AKT/mTOR and MAPK Signaling Pathways in
903 Colorectal Cancer Pathogenesis: Where Are We Now? *Int J Mol Sci*. **22,** 10260 (2021).
904 44. Wang, Y.P. et al., Insulin receptor tyrosine kinase substrate activates EGFR/ERK
905 signalling pathway and promotes cell proliferation of hepatocellular carcinoma. *Cancer*
906 *Lett*. **337,** 96-106 (2013).
907 45. Zunke, F. & Rose-John, S., The shedding protease ADAM17: Physiology and
908 pathophysiology. *Biochim Biophys Acta Mol Cell Res*. **1864,** 2059-2070 (2017).
909 46. Scapin, G. et al., Structure of the insulin receptor-insulin complex by single-particle
910 cryo-EM analysis. *Nature*. **556,** 122-125 (2018).
911 47. Kotani, N. et al., Biochemical visualization of cell surface molecular clustering in living
912 cells. *Proc Natl Acad Sci USA.* **105,** 7405-9 (2008).
913 48. Kotani, N. et al., Proximity proteomics identifies cancer cell membrane cis-molecular
914 complex as a potential cancer target. *Cancer Sci.* **110**(8)**:** 2607-2619 (2019).

915 49. Kobayashi, S. et al., EGFR Mutation and Resistance of Non–Small-Cell Lung Cancer
916 to Gefitinib. *N Engl J Med*. **352,** 786-792 (2005).
917 50. Kumagai, S., Koyama, S., Nishikawa, H., Antitumour immunity regulated by aberrant
918 ERBB family signalling. *Nat Rev Cancer*. **21**, 187-197 (2021).
919 51. Sawasaki, T., Ogasawara, T., Morishita, R., Endo, Y., A cell-free protein synthesis
920 system for high-throughput proteomics. *Proc. Natl Acad. Sci. USA* **99**, 14652–14657
921 (2002).
922 52. Nagase, T. et al., Exploration of human ORFeome: high-throughput preparation of ORF
923 clones and efficient characterization of their protein products. *DNA Res.* **15**, 137–149
924 (2008).
925 53. Jumper, J. et al., Highly accurate protein structure prediction with AlphaFold. *Nature*.
926 **596**, 583-589 (2021).
927 54. Law, A.M.K. et al., Andy's Algorithms: new automated digital image analysis pipelines
928 for FIJI. *Sci Rep*. **7,** 15717 (2017).
929

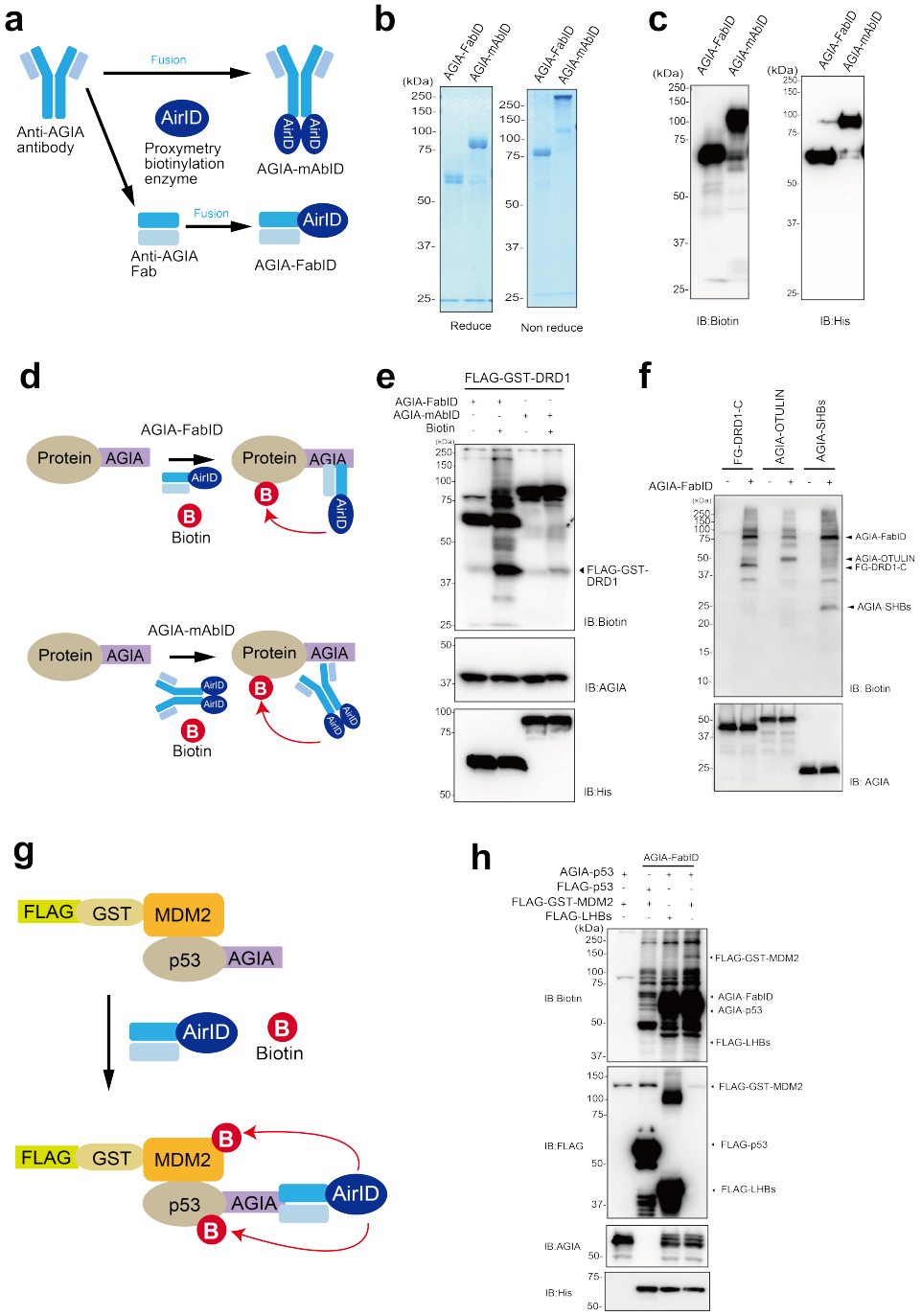

930

931 **Fig. 1: Biotinylation of AGIA-tag protein by AGIA-FabID and AGIA-mAbID.**

932 **a,** Schematic of AGIA antibody fused with the proximity biotinylation enzyme AirID.
933 AirID is fused to AGIA-Fab or AGIA-mAb, **b,** SDS-PAGE and Coomassie Brilliant Blue
934 (CBB) staining in reducing and non-reducing state of AGIA-FabID and AGIA-mAbID

synthesized by Expi293F expression system and purified by Ni Sepharose excel. **c,** Detection of self-biotinylation of AGIA-FabID and AGIA-mAbID by western blotting using an anti-biotin antibody. **d,** Schematic of biotinylation targeting the AGIA-tagged protein using AGIA-FabID and AGIA-mAbID. **e,** Comparison of the activities of AGIA-FabID and AGIA-mAbID targeting FLAG-GST-DRD1(C-terminal*) in vitro*. **f,** Targeting various AGIA-tagged proteins biotinylated by AGIA-FabID. **g,** Schematic of the biotinylation-targeting complex of p53-MDM2 using AGIA-FabID. **h,** Confirmation of biotinylation of FLAG-GST-MDM2 and AGIA-p53 by western blotting.

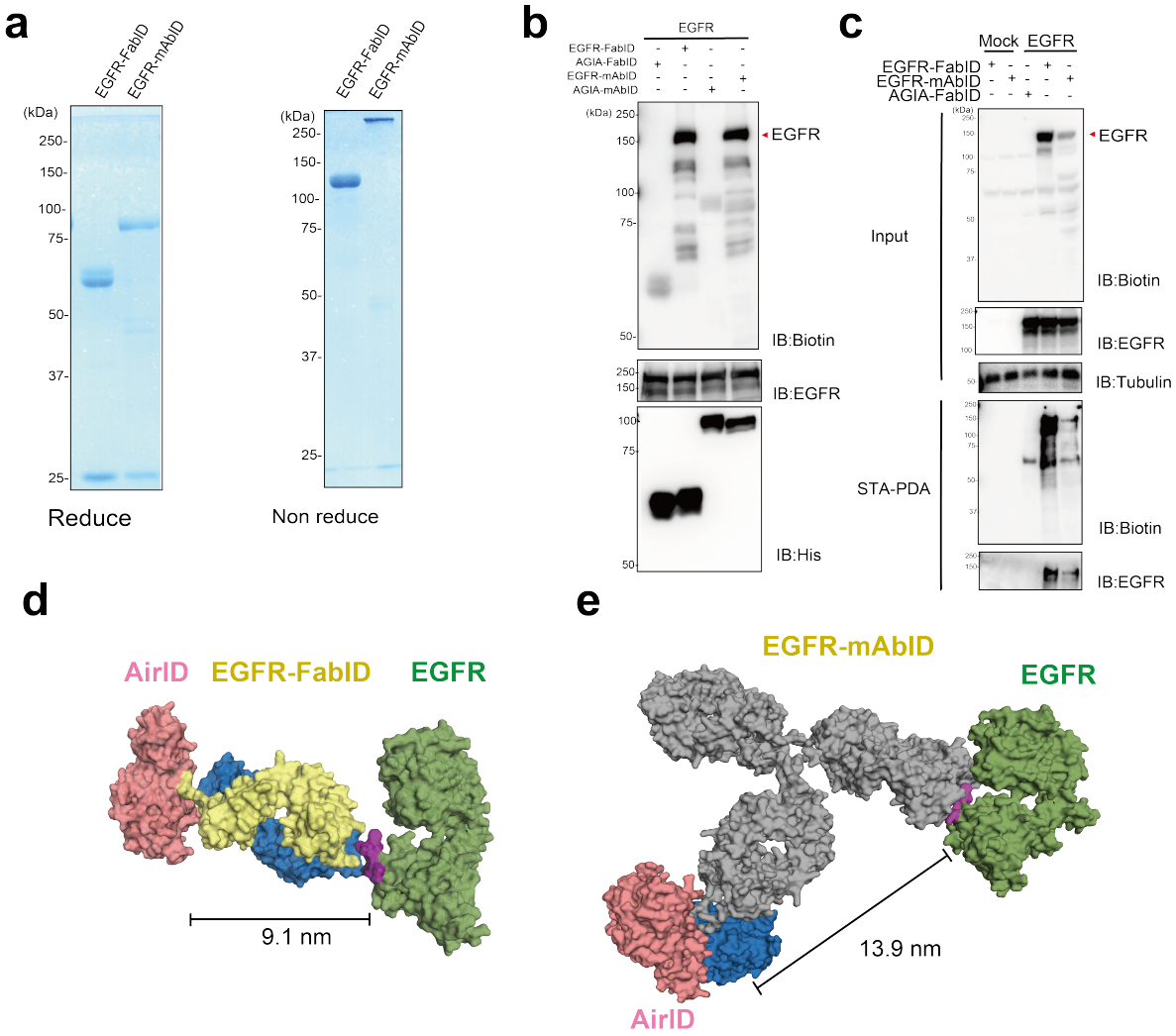

f

Region	Biotinylation site (K)	Distance from Ser380 (nm)
Extracellular	133	4.5
	479	4.5
	454	4.5
	487	3.1
	489	4.2
Intracellular	716	
	745	
	754	
	739	
	846	
	852	
	1188	

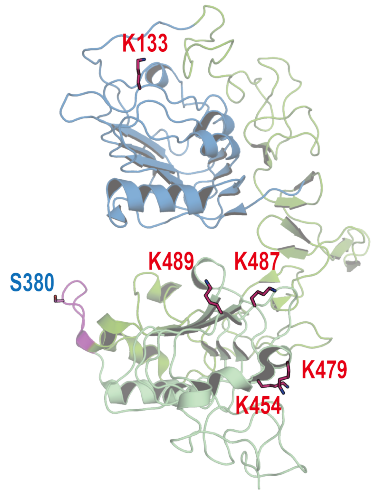

Fig. 2: Biotinylation analysis of EGFR by EGFR- FabID on the cell membrane.

a, SDS-PAGE of EGFR-FabID and EGFR-mAbID synthesised by the Expi293F expression system, purified by Ni Sepharose in reducing and non-reducing states, and stained with CBB. **b,** Biotinylation of EGFR using EGFR-FabID and EGFR-mAbID *in vitro*. EGFR was synthesised using a wheat cell-free protein synthesis system-based Disulfide Bond PLUS Expression Kit. **c,** Immunoblot analysis of EGFR biotinylated by EGFR-FabID and EGFR-mAbID on the plasma membrane using EGFR-overexpressing Expi293F cells. **d,** EGFR-FabID modelling diagram calculated from structural information and AlphaFold. Green represents EGFR, and yellow and blue represent anti-EGFR Fab. Pink represents AirID. **e,** EGFR-mAbID modelling diagram calculated from structural information and AlphaFold. Green represents EGFR; grey, and blue represent anti-EGFR mAbs. Pink represents AirID. **f,** Biotinylation site of EGFR detected by LC-MS/MS; the intermolecular distance between S380 of EMab-134 epitope and biotinylated lysine residue was measured by PyMOL based on structural information (PDB 1IVO) and **g,** biotinylation sites of extracellular domain EGFR.

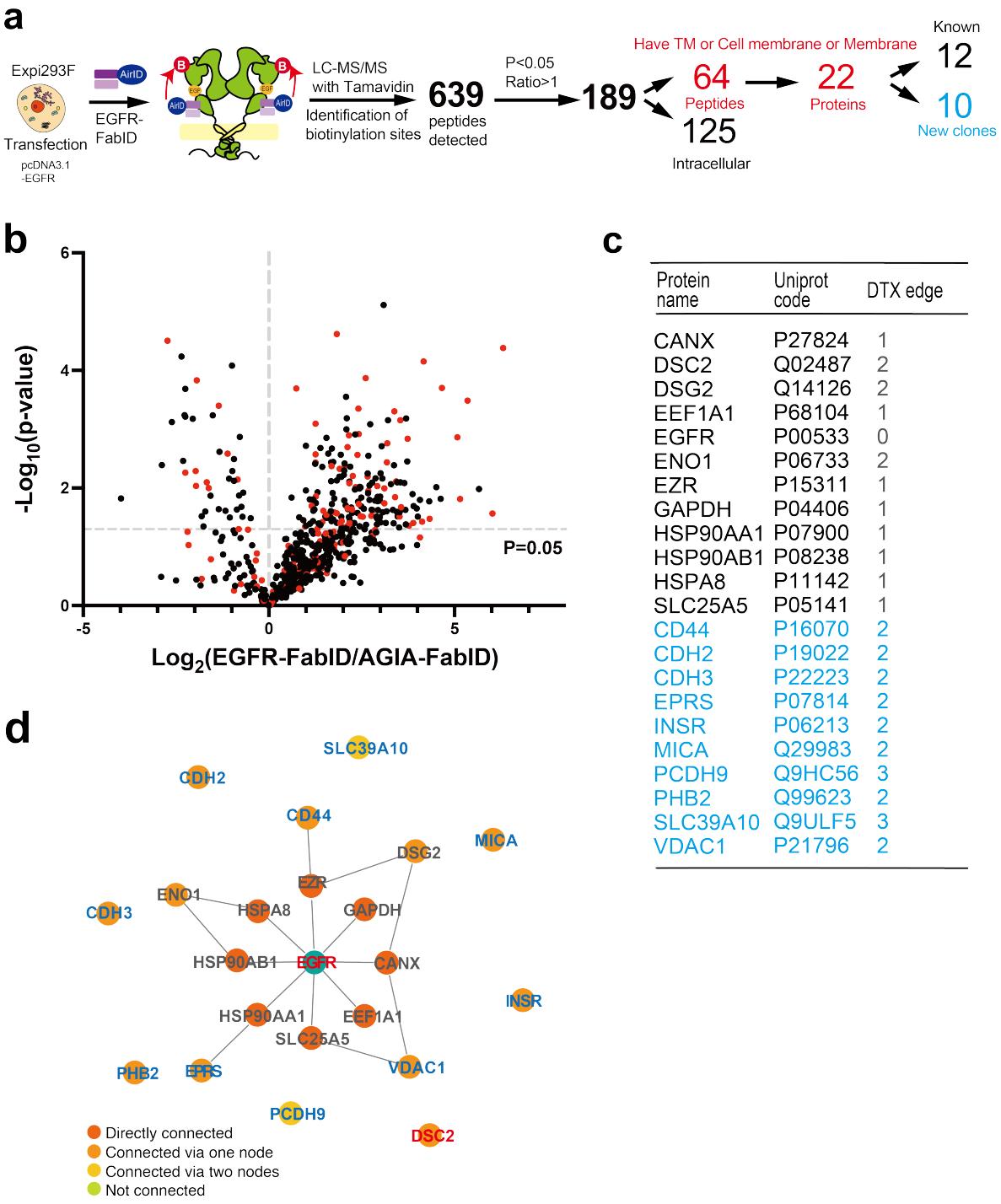

Protein name	Uniprot code	DTX edge
CANX	P27824	1
DSC2	Q02487	2
DSG2	Q14126	2
EEF1A1	P68104	1
EGFR	P00533	0
ENO1	P06733	2
EZR	P15311	1
GAPDH	P04406	1
HSP90AA1	P07900	1
HSP90AB1	P08238	1
HSPA8	P11142	1
SLC25A5	P05141	1
CD44	P16070	2
CDH2	P19022	2
CDH3	P22223	2
EPRS	P07814	2
INSR	P06213	2
MICA	Q29983	2
PCDH9	Q9HC56	3
PHB2	Q99623	2
SLC39A10	Q9ULF5	3
VDAC1	P21796	2

Fig. 3: Proximity extracellular interactome of over-expressing EGFR by EGFR-FabID on cells.

a, Workflow of PPI analysis targeting EGFR overexpression. LC-MS/MS identified 640 biotinylated peptides, of which 189 were selected as those with AGIA-FabID ratios > 1 and $P < 0.05$. The number of peptides was then narrowed to 64 peptides that had transmembrane (TM) regions or contained "membranes" in the gene ontology (GO) term. 64 peptides were matched into 22 proteins. Twelve of the 22 proteins were known to interact with EGFR, and 10 were novel EGFR-interacting proteins. **b,** Volcano blot (3 biological replicates) of peptides detected as biotinylated peptides by LC-MS/MS in **a**. Peptides derived from cell membrane proteins are indicated by red dots. **c,** Table of extracellular proteins identified by mass spectrometry (three biological replicates, EGFR-FabID/AGIA-FabID ratios > 1 and $P < 0.05$). The number of DTX edges for each protein and EGFR are shown in the table. Proteins in black font are those already known to interact with EGFR, whereas those in blue represent new EGFR-interacting proteins. **d,** EGFR interaction was detected using AlphaScreen (three technical replicates). Alphascreens with the EGFR extracellular domain and various FLAG fusion proteins. **e,** Pathway analysis of extracellular proteins detected using mass spectrometry. The Gene Ontology software Drug Target Excavator (DTX) (https://harrier.nagahama-i-bio.ac.jp/dtx/) and IntAct database, including EGFR-interacting proteins (https:///ebi.ac.uk/intact/), were used to analyse protein interactions.

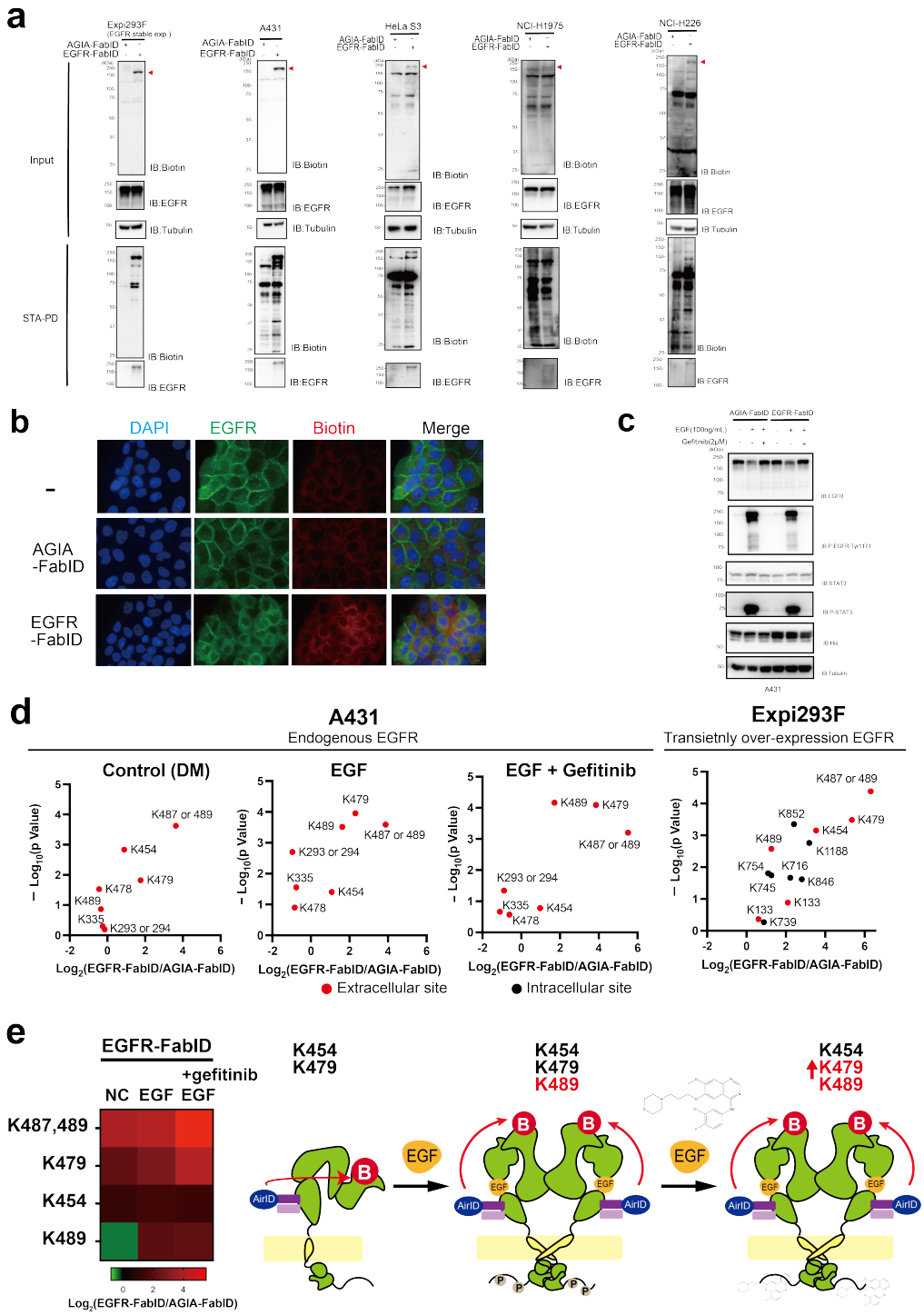

983

984 **Fig. 4: Biotinylation analysis of endogenous EGFR by EGFR-FabID in human A431**

985 **cells.**

a, Streptavidin pull-down assay of endogenous EGFR on the plasma membrane biotinylated by EGFR-FabID in various cells. Red arrowheads indicate the molecular weight of EGFR. **b,** Immunostaining with EGFR-FabID in A431 cells. Control-treated areas included those without FabID treatment and those treated with AGIA-FabID. **c,** Kinase assay using A431 and NCI-H226 cells. Phosphorylation of EGFR and STAT3 activated by EGF stimulation was then confirmed using western blotting. **d,** Volcano plot of biotinylated EGFR peptides identified by mass spectrometry (three biological replicates). Red dots represent peptides derived from the extracellular domain of EGFR, and black dots represent peptides derived from the intracellular domain. **e,** Heat map showing changes in biotinylated peptide sites upon EGF and gefitinib treatment of A431 cells (three biological replicates). Schematic of the changes in the EGFR biotinylated site.

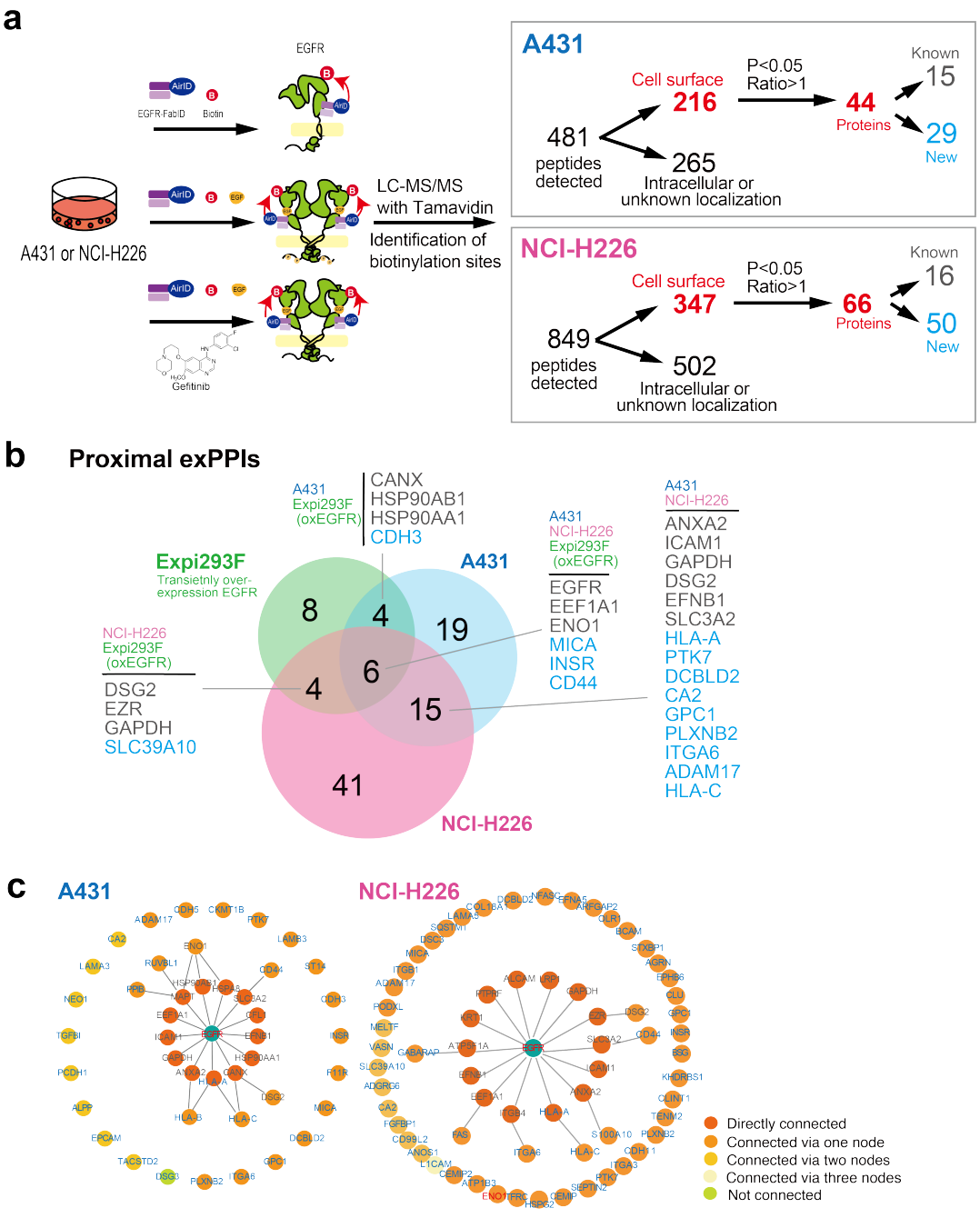

Fig. 5: Total proximity extracellular biotinylation analysis of EGFR using EGFR-FabID in A431 and NCI-H226 cells with or without EGF ligand and/or gefitinib.

a, Workflow of PPI analysis targeting A431 cells. The same procedure as that in Fig. 3 was used to narrow down the peptides to extracellular peptides. As a result, 216 peptides in A431 cells and 347 peptides in NCI-H226 cells were derived from cell surface peptides. In A431 cells, 15 molecules were known to interact with EGFR, and 29 molecules were novel interacting proteins. In NCI-H226 cells, 16 molecules were known to interact with EGFR, and 50 molecules were novel interacting proteins. **b,** Venn diagram of proteins predominantly biotinylated in EGFR-overexpressing Expi293F, A431, and NCI-H226 cells. The numbers represent the number of proteins in the region (EGFR-FabID/AGIA-FabID ratios > 1 and $P < 0.05$). **c,** Pathway analysis of 44 proteins in A431 cells and 66 proteins in NCI-H226 cells, obtained from workflow shown in Fig 5a.

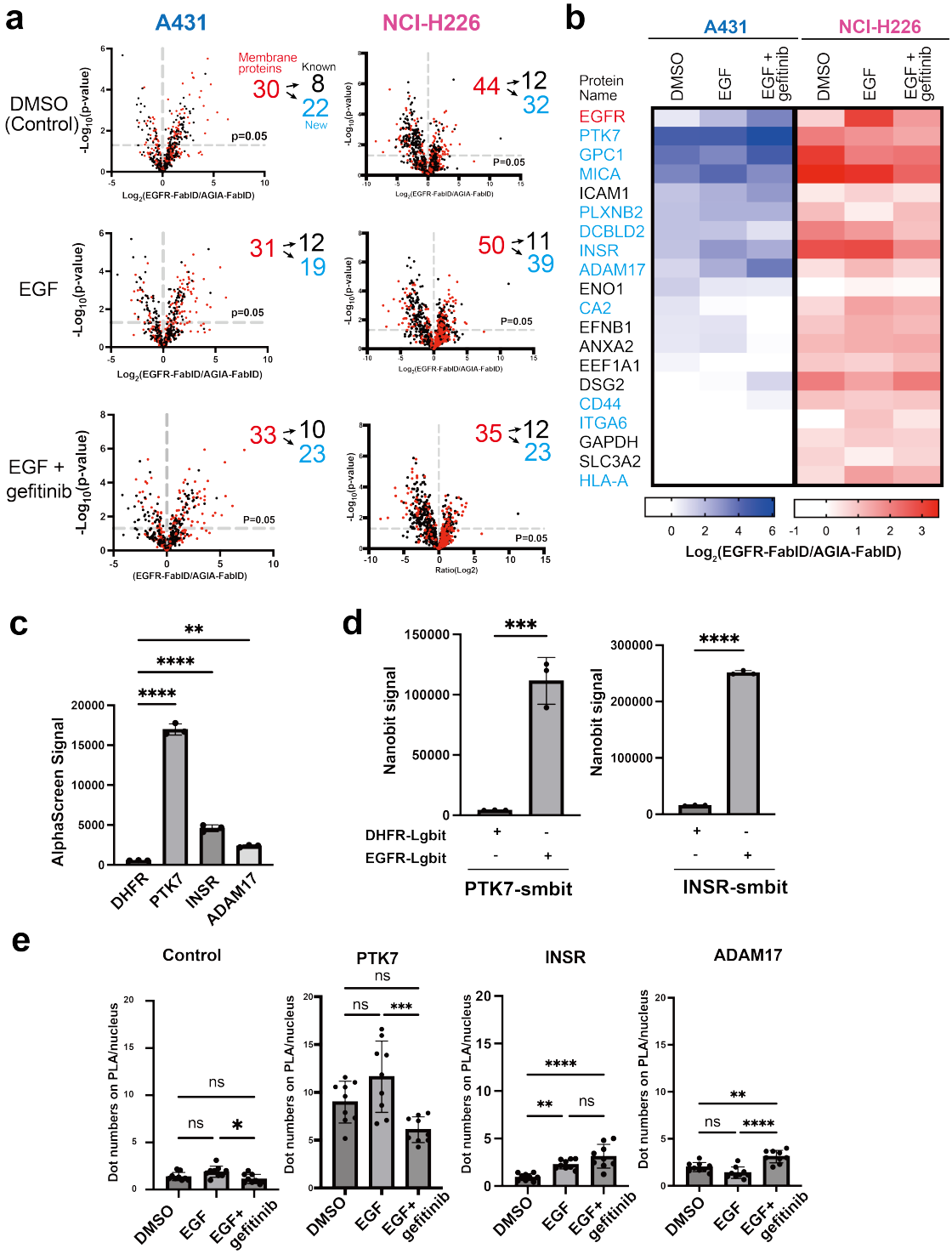

Fig. 6: Individual analysis of exPPI response to EGFR in A431 and NCI-H226 cells in the presence of EGF and gefitinib.

a, Volcano plot of DMSO (Control) EGF- or EGF+gefitinib-treated zones, each detected as biotinylated peptides by LC-MS/MS. Peptides derived from plasma membrane proteins are indicated by red dots (three biological replicates). Numbers in black indicate the number of proteins known to interact with EGFR. Numbers in blue indicate the number of proteins that are novel interactors with EGFR. **b,** Heat map showing exPPI changes upon addition of EGF or gefitinib for cell surface proteins that were commonly biotinylated in A431 and NCI-H226 cells (three biological replicates). **c,** EGFR interactions were detected using AlphaScreen (three technical replicates). AlphaScreen with the EGFR extracellular domain and various FLAG fusion proteins. Statistical significance was determined using one-way ANOVA (****$P \leq 0.0001$, ***$P \leq 0.0002$, **$P \leq 0.0021$). **d,** Confirmation of live-cell interactions using the NanoBiT system. A DHFR-Lgbit was used as the control. Statistical significance was determined using one-way analysis ANOVA (****$P \leq 0.0001$, ***$P \leq$ 0.0002). **e,** Bar graph depicting the number of PLA-positive foci compared to each treatment group calculated with Andy's PLA algorithm and quantified using GraphPad Prism 9 software (n=9 per group, t-test One-way ANOVA(****$P \leq 0.0001$, ***$P \leq 0.0002$, **$P \leq 0.0021$, *$P \leq 0.0332$).

Supplementary Files

This is a list of supplementary files associated with this preprint. Click to download.

- DescriptionofAdditionalSupplementaryFiles.docx
- YamadaSupplementaryInformation.pdf
- Supplementarytable4EGFRFabID.xlsx
- Supplementarytable5EGFRFabID.xlsx
- Supplementarytable1EGFRFabID.xlsx
- Supplementarytable2EGFRFabID.xlsx
- Supplementarytable3EGFRFabID.xlsx
- YamadaSupplementaryInformation.pdf
- SourceDataEGFRFabID.xlsx